PNAS RESEARCH ARTICLE | ECOLOGY

Terrestrial ecosystem nitrogen cycling in response to field warming: Global patterns and future trends

Xudong Wang[a,b], Chenrui Ni[b], Ziyi Fan[b], Wenao Wu[b], Changlin Xu[b], Jiguang Feng[a], Rui Yin[c], Joshua P. Schimel[d], Margaret S. Torn[e,f], and Biao Zhu[a,b,1]

Affiliations are included on p. 9.

Edited by James Ehleringer, The University of Utah, Salt Lake City, UT; received November 13, 2025; accepted January 28, 2026

Nitrogen cycling regulates terrestrial ecosystem productivity and carbon sequestration, yet its response to climate warming remains uncertain. Here, we compiled the most comprehensive dataset to date, integrating 7,941 observations from 413 field warming experiments worldwide with random forest regression and Community Land Model (CLM) simulations. Field warming significantly accelerated nitrogen cycling, increasing N_2O emissions (+24.7%), mineralization (+25.8%), nitrification (+51.7%), and denitrification (+41.1%). Soil inorganic nitrogen also increased, while plant nitrogen remained largely unchanged. Elevated natural abundance of ^{15}N indicated that warming alleviates nitrogen limitation and promotes more open nitrogen cycles. Soil moisture, ecosystem type, and warming magnitude were key drivers. N_2O emission and nitrification further intensified with increased warming magnitude in random forest analyses. In contrast, CLM5-BGC simulated weak responses in N_2O emissions and nitrification and negative changes in nitrogen mineralization, substantially diverging from field observations. These discrepancies highlight the omission of microbial processes and the oversimplification of large-scale ecosystem feedbacks, respectively. Uniquely, this study provides a direct comparison among empirical data, random forest regression, and CLM simulations, revealing discrepancies and their potential causes. Collectively, our findings demonstrate that terrestrial nitrogen cycling is more responsive to climate warming than previously recognized and underscore the importance of integrating multiple analytical approaches to synthesize cross-scale ecological data.

field warming | nitrogen cycling | meta-analysis | community land model

Significance

Nitrogen cycling regulates ecosystem productivity and carbon storage, yet its global responses, mechanisms, and future trajectories under climate warming remain poorly understood. By integrating 7,941 observations from 413 field warming experiments with random forest regression and Community Land Model (CLM) simulations, we conducted a cross-scale synthesis of nitrogen cycling responses to warming. Warming consistently accelerates key nitrogen transformations (including mineralization, nitrification, denitrification, and N_2O emissions), thereby alleviating nitrogen limitation across ecosystems. Uniquely, this study provides a direct comparison among empirical data, random forest regression, and CLM simulations, revealing discrepancies and underlying causes. Our findings demonstrate that terrestrial nitrogen cycling is more dynamic under climate warming than previously recognized, with important implications for projecting carbon–nitrogen interactions in ecosystem models.

Nitrogen (N), an essential basic element for all life, crucially shapes ecosystem structure and function (1). Its availability regulates carbon sequestration, with far-reaching implications for global food security and environmental health (2, 3). Climate warming, projected to increase terrestrial surface temperatures by 2.4 to 4.8 °C by the end of this century (4), profoundly transforms ecosystem N cycling and poses substantial threats to global ecosystems and human sustainability. Crucially, these changes can significantly increase emissions of nitrous oxide (N_2O). N_2O is a potent, long-lived greenhouse gas (GHG), with a radiative efficiency 273 times that of CO_2 at a 100-y time horizon (5). In 2020 and 2021, the atmospheric growth rate of N_2O exceeded 1.3 ppb y^{-1}, the highest rate observed since 1980 (6). These trends underscore the urgency of understanding how climate warming influences terrestrial N cycling. Mechanistically, elevated temperatures enhance key aspects of N cycling: they boost foliar N uptake efficiency, intensify N resorption, and improve root N acquisition capacity (7, 8). Warming also accelerates soil N mineralization (9, 10), stimulates microbial N fixation, and promotes mycorrhizal-mediated nutrient transfer (11, 12), thereby increasing belowground N availability. Collectively, these processes increase the risk of enhanced gaseous N losses and could initiate positive feedback loops: Increased N_2O emissions exacerbate climate forcing, which in turn may further accelerate ecological degradation through enhanced warming and altered N cycling (13, 14). Therefore, understanding ecosystem responses to warming-induced perturbations in N cycling is critical for developing predictive frameworks capable of simulating future terrestrial N flux trajectories.

Field-based manipulative warming experiments are a fundamental approach for investigating N cycle dynamics, and as early as the 1990s, researchers had already conducted *pioneering* studies in this area (15, 16). Advances in experimental warming technologies and in situ measurement techniques have greatly expanded this field, resulting in a steady increase in related publications over the past three decades. These developments have established warming–N interaction studies as a central theme in global change and biogeochemical cycling. However, findings remain dispersed across numerous studies

The authors declare no competing interest.

This article is a PNAS Direct Submission.

[1]To whom correspondence may be addressed. Email: biaozhu@pku.edu.cn.

This article contains supporting information online at https://www.pnas.org/lookup/suppl/doi:10.1073/pnas.2532868123/-/DCSupplemental.

Published February 25, 2026.

conducted across ecosystem types using various warming methods, complicating cross-site comparisons and synthesis. To overcome these challenges, recent efforts have increasingly relied on integrated analyses and modeling approaches to assess N cycle responses to warming across broader spatial and temporal scales. Key findings from these studies include soil N_2O and other greenhouse gas emissions tend to increase with warming magnitude but decline with prolonged warming duration (17); In high-latitude ecosystems, warming enhances N mineralization and N_2O emissions, while promoting accumulation of dissolved organic N and root N (18). In these environments warming increases soil and foliar N content, but has a minor effect on microbial biomass nitrogen (MBN) (13); warming also does not significantly alter the abundance of most N-cycling functional genes (19). In Arctic soils, DON, NH_4^+, and NO_3^- levels were unaffected by warming, but increased markedly with snow addition (20). Shoot N content generally increases under warming, whereas other plant tissues, soils, and MBN show no significant changes (21). In grasslands, warming intensified N dynamics, increasing primary productivity but also promoting N loss to the environment (22). A comparison of our current study with previous syntheses on N cycling (based on research scale, data type, and methodology) is provided in *SI Appendix*, Table S1.

Despite these advances, current syntheses face two critical limitations: First, limited data coverage and inconsistent metrics constrain robust quantification of the magnitude and variability of global patterns in warming-driven N cycling changes. Second, insufficient mechanistic understanding across diverse ecosystems hinders the identification of key drivers governing these responses and limits systematic integration of existing findings. Consequently, a comprehensive understanding of how warming reshapes the terrestrial N cycle remains elusive. To address these gaps, we believe this study has established the most comprehensive dataset to date and presents a global synthesis of three decades of field-based in situ experimental data on terrestrial N cycling responses to warming. Through a comprehensive analytical framework incorporating meta-analysis techniques, random forest modeling, spatial pattern analysis, and process-based modeling, we systematically addressed: 1) the response patterns, key drivers, and mechanisms of major N cycling components (including N fluxes, transformation processes, soil N, and plant N) under experimental warming; 2) global patterns and future trajectories of N fluxes and transformations under climate change scenarios, and 3) are there any differences between the model and the experimental results. We tested the following hypotheses: (H1) Experimental warming will significantly accelerate N_2O emissions, N mineralization, and nitrification rates, which are mainly regulated by soil water content, warming magnitude, and ecosystem type. (H2) As climate warming intensifies in the future, N_2O emissions and N transformations should increase, but the magnitude and spatial patterns of these responses may differ among process-based model, meta-analysis, and mapping.

Results and Discussion

Warming Accelerates N_2O Emission and Nitrogen Transformation. Consistent with Hypothesis 1, our global-scale meta-analysis (Fig. 1) confirms that field warming experiments significantly increased the rate of N_2O emissions (quantified as the response ratio, RR), with a weighted mean effect size of +24.7% (hereafter, all effect sizes refer to weighted means). Warming also markedly enhanced soil N mineralization (+25.8%), nitrification (+51.7%), and denitrification (+41.1%) rates. In contrast, N fixation showed no significant change (–25.2%, 95% CI: –114.8 to 64.4%). Two mechanisms have been proposed to explain the observed acceleration of N transformations under elevated temperatures (2, 23–26). First, warming enhances the decomposition of organic N, increasing the availability of inorganic N, which in turn stimulates nitrification, denitrification, and associated N_2O emissions. Second, warming-induced changes in biological activity and soil moisture may alter soil oxygen availability, indirectly facilitating N transformation. Furthermore, soil N dynamics are further modulated by site-specific factors, including soil type, environmental condition, and microbial community composition.

Next, we conducted model selection and metaregression analyses to examine the responses of three key nitrogen-cycling indicators (N_2O emissions, nitrogen mineralization rates, and nitrification rates) to warming (Fig. 2). The results showed that ΔSWC (calculated as the difference in soil water content between warmed and control plots, with negative values indicating soil drying after warming and positive values indicating soil wetting) was the most important predictor, while variation in warming magnitude (ΔT) and experimental duration also influenced these core nitrogen-cycling responses. To evaluate spatial patterns, we

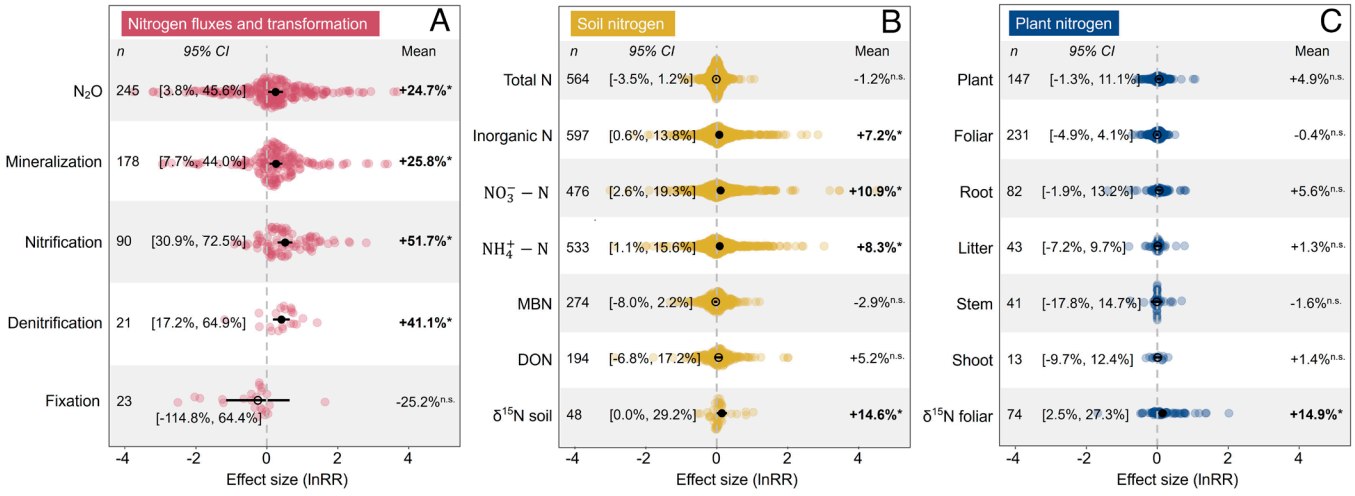

Fig. 1. Effects of warming (calculated as the response ratio, RR) on the nitrogen (N) fluxes and transformations (*A*), soil N (*B*), and plant N (*C*). The vertical dashed line denotes a response ratio of zero. n indicates the number of observations. Error bars represent 95% CI. Solid points and bold means represent significant warming effects (95% CI does not overlap zero); hollow points and nonbold means indicate nonsignificant effects. Each scatter point shows an individual observation. MBN: microbial biomass nitrogen; DON: dissolved organic nitrogen.

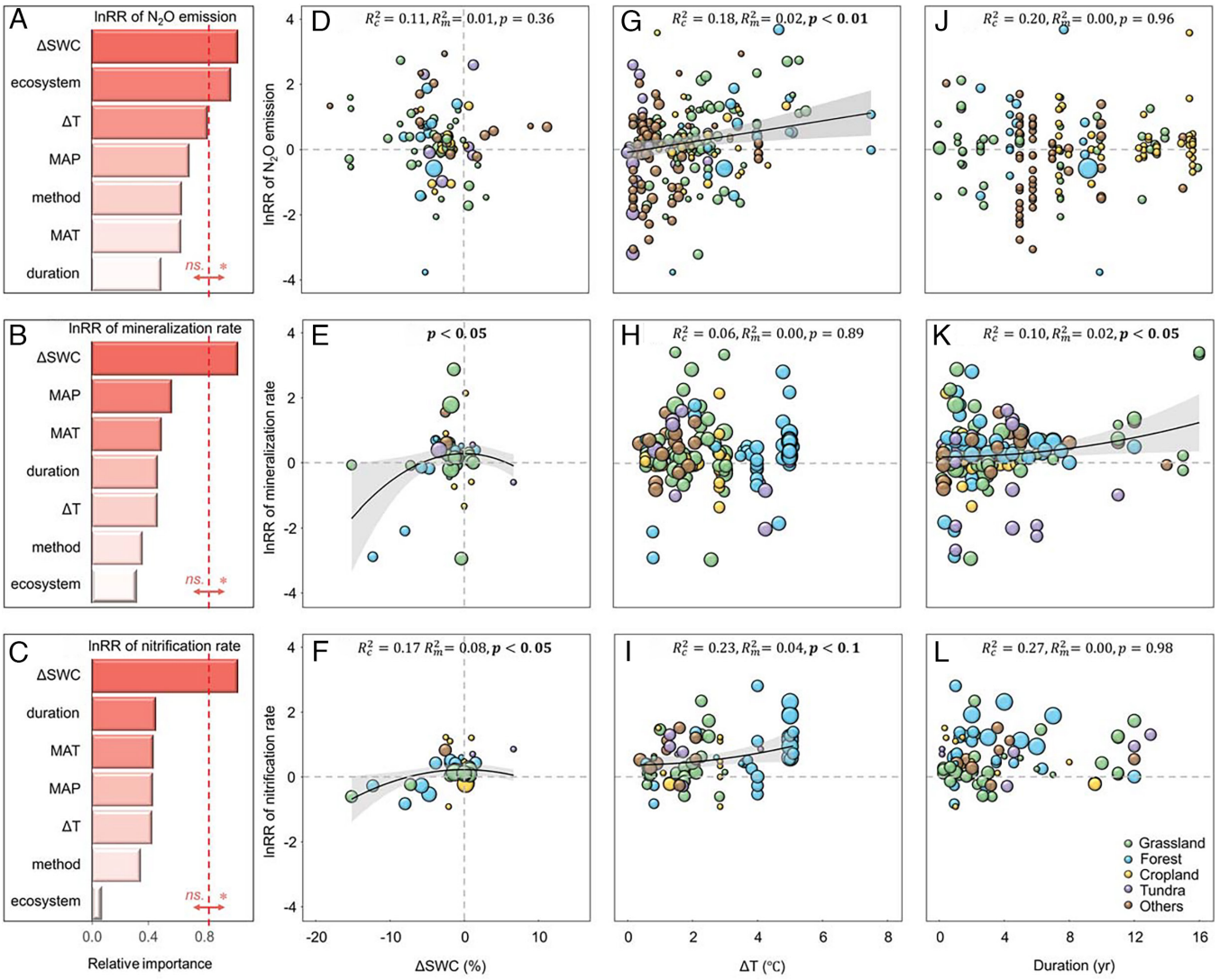

Fig. 2. Determinants of warming effects on N_2O emissions, nitrogen mineralization, and nitrification rates (calculated as the response ratio, RR). (*A–C*) Relative importance of predictors based on the sum of Akaike weights from model selection using corrected Akaike's Information Criterion (AICc). Predictors with weights ≥ 0.8 are considered influential. Variables include: duration (experimental duration), MAP (mean annual precipitation), MAT (mean annual temperature), method (warming method), ecosystem (ecosystem type), ΔT (warming magnitude), and ΔSWC (change in soil water content). (*D–L*) Metaregression results showing relationships between response ratio (RR) and ΔSWC, ΔT, and duration. Point size indicates data weight (number of observations); the shaded area shows 95% CI. Colored dots denote ecosystems: grassland (green), forest (blue), cropland (yellow), tundra (purple), others (brown; includes wetland, shrubland, heathland, etc.). Marginal R^2 (*m*) and conditional R^2 (*c*) represent variance explained by fixed effects and by both fixed and random effects (site), respectively.

generated data-derived global maps of warming effects under +2 and +4 °C scenarios (Fig. 3). Compared to +2 °C warming (+20.0%, Fig. 4*A*), the RR of N_2O emissions under +4 °C increased markedly to +30.0% ($P < 0.01$), consistent with Hypothesis 2, indicating a substantial escalation with intensified warming. The RR of nitrification rates rose from +32.6% (+2 °C) to +47.0% (+4 °C) (Fig. 4*G*, $P < 0.001$), whereas the RR of N mineralization showed a slight decline (+21.5% vs. +19.3%) (Fig. 4*D*, $P > 0.05$). In general, warming increases the abundance of N-cycling genes, thereby accelerating N transformation processes (27). However, with further increases in warming, the energetic and resource demands required to sustain microbial activity and function also rise. This may suppress the activity of hydrolytic enzymes involved in carbon and N metabolism, and ultimately, multiple factors jointly constrained mineralization rates (28, 29). This is consistent with Fig. 2*H*, indicating that there is no significant correlation between the RR of mineralization rate and warming magnitude. By contrast, N_2O emissions and nitrification rates were both significantly positively correlated with warming magnitude (Fig. 2 *G* and *I*), leading to asynchronous responses among N_2O emissions, nitrification, and nitrogen mineralization as warming intensity increased.

Subgroup analyses revealed that experiments using OTC (open-top chamber) did not show significant changes in the response of N_2O emissions, mineralization, or nitrification, whereas active warming methods, such as HC (heating cable), resulted in significant increases (*SI Appendix*, Fig. S1 *E–G*). This might be related to the fact that the average warming depth and magnitude of HC (9.1 cm, 4.2 °C) in this dataset are higher than those of OTC (5.8 cm, 1.3 °C). The response of N_2O emissions to warming is influenced by multiple factors, including vegetation composition, soil moisture, nutrient availability, and soil properties (30–32). Among these, the availability of mineral N, modulated by plant N uptake, is the principal driver of soil N_2O emissions (33, 34). Current field warming experiments are mainly concentrated in grasslands, forests, and croplands. However, regions and ecosystems with stronger climate warming trends or more organic N accumulation, such as the Arctic and subarctic

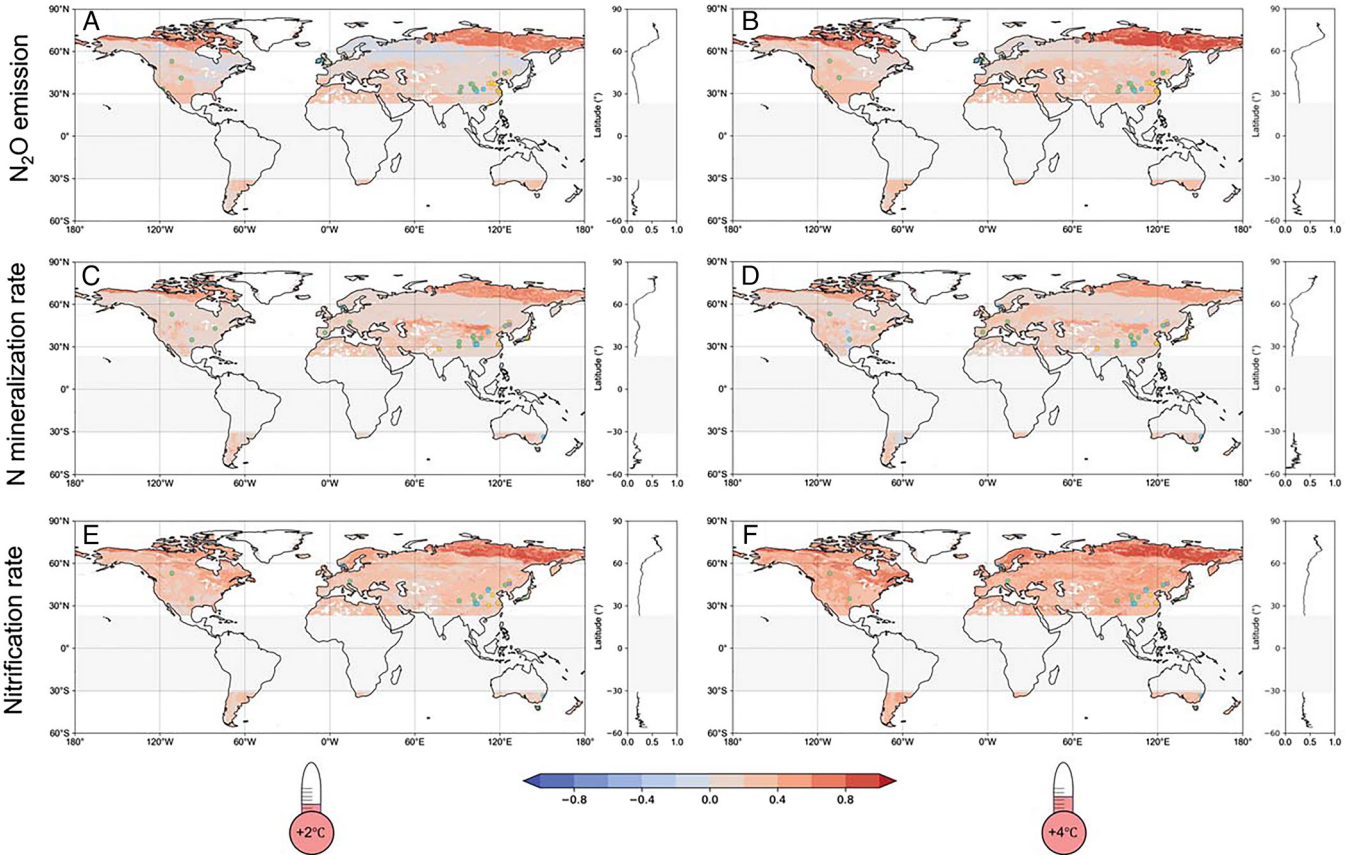

Fig. 3. Global mapping of the natural logarithm of the response ratio (lnRR) of N_2O emission (*A* and *B*), nitrogen mineralization rate (*C* and *D*), and nitrification rate (*E* and *F*) under 2 and 4 °C warming. The *Right* panel of each plot shows the change of averaged values along the latitudinal gradient. Legend values represent the average change rates per 0.042° × 0.042° grid. Source data are provided as a Source Data file. The gray area (31°S to 23°N) indicates regions with a lack of corresponding data. The colored dots represent the original studies used for mapping (grassland, green; forest, blue; cropland, yellow; tundra, purple; others, includes wetland, shrubland, heathland, etc., brown).

regions and permafrost peatland, may respond more strongly to climate change and have higher N_2O emission potential, which deserves more attention (35–37).

As biological N fixation represents a major N input to ecosystems, the presence of N-fixing plants may modulate ecosystem N cycling responses to warming. We conducted subgroup analyses based on the presence or absence of N-fixing species. The results showed that warming significantly increased the response of N_2O emissions, mineralization, and nitrification only in ecosystems without N-fixers, whereas no significant changes were observed in ecosystems with N-fixers (*SI Appendix*, Fig. S2 *A*–*C*). Several mechanisms may explain this (38–40): 1) soils in N-fixer–dominated ecosystems tend to have higher ammonium (NH_4^+) concentrations, which are more readily adsorbed by soil colloids than nitrate (NO_3^-), thereby reducing N_2O production; 2) N-fixing trees typically require substantial N uptake to sustain their N-rich biomass, which can deplete available soil N and constrain N_2O emissions; 3) Ecosystems with N-fixing plants may regulate N_2O dynamics through integrated changes in soil carbon and N pools, water-use efficiency, and other traits, all of which are influenced by species-specific N-fixation strategies and background N deposition rates, making the response highly context-dependent. 4) Under high nitrogen availability from N-fixers, ecosystems may experience a shift from nitrogen limitation to colimitation by other factors (e.g., phosphorus, moisture, or soil acidity). These factors exhibit lower temperature sensitivity compared to nitrogen-scarce conditions, thereby dampening the warming response of N_2O emissions.

Divergent Results of Process-Based Model, Meta-Analysis, and Mapping. Simulation results from the Community Land Model (CLM) version 5.0 with Biogeochemistry (CLM 5-BGC) predict that by the end of this century, N_2O emissions rise by 8.2% and 15.8% under prescribed warming scenarios of +2 and +4 °C, respectively (Fig. 4*C* and *SI Appendix*, Fig. S3, $P < 0.05$), while nitrification rates rise by 6.9% and 24.1% (Fig. 4*I*, $P < 0.05$). These increases are substantially smaller than those revealed by our meta-analysis (Fig. 1*A*) and random forest mapping (Figs. 3 and 4). Moreover, CLM5-BGC simulates a decline in N mineralization rates (–8.54 and –8.48% under +2 and +4 °C scenarios, respectively; Fig. 4*F*, $P > 0.05$), which contrasts with both empirical evidence and synthesis results. One possible reason is that these simulations applied uniform step-wise temperature perturbations (+2 and +4 °C), rather than transient future climate trajectories characterized by gradual warming. Experimental and theoretical evidence suggests that abrupt, sustained warming can trigger strong initial microbial responses followed by acclimation and substrate limitation (41), whereas gradual warming may lead to more progressive adjustments in microbial activity and nitrogen cycling. As a result, differences in warming trajectories may contribute to the divergence between model simulations and empirical observations. More importantly, the divergence suggests that key microbial processes may be underrepresented in current models and some soil processes may be oversimplified in experimental warming designs.

Soil microbial communities adapt to warming through shifts in community composition, such as the enrichment of thermotolerant and thermophilic taxa, or through physiological adjustments,

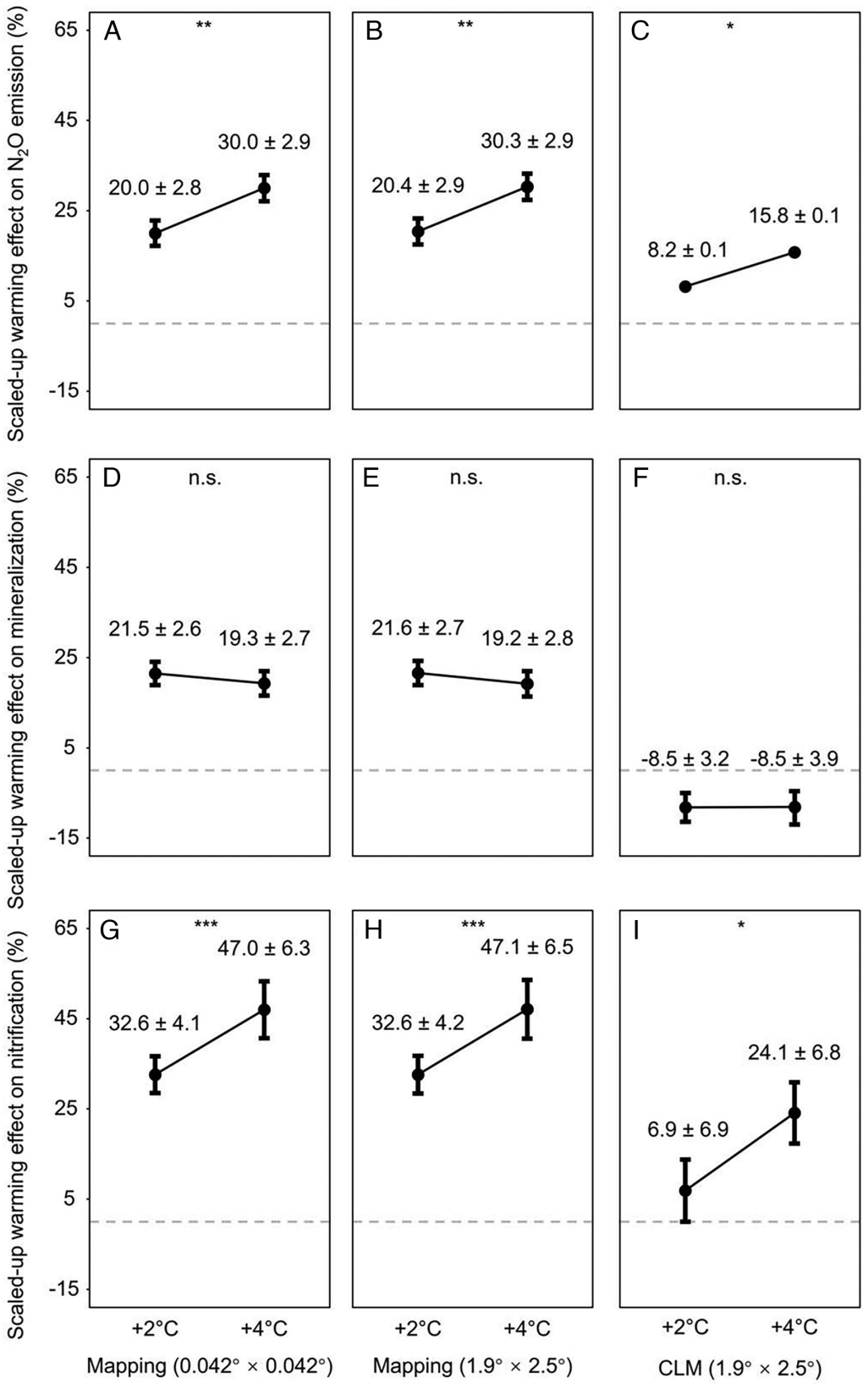

Fig. 4. Scaled-up warming effect (mean ± SD) on the responses of N_2O emission (*A*–*C*), N mineralization (*D*–*F*), and nitrification (*G*–*I*) under +2 and +4 °C warming scenarios compared to baseline (%). (*A*, *D*, and *G*): global mapping at a spatial resolution of 0.042° × 0.042°, (*B*, *E*, and *H*): global mapping at a spatial resolution of 1.9° × 2.5°, (*C*, *F*, and *I*): Community Land Model (CLM) version 5.0 with Biogeochemistry at a spatial resolution of 1.9° × 2.5°. ***$P < 0.001$, **$P < 0.01$, *$P < 0.05$, n.s.: $P > 0.05$.

including elevated enzyme production (42). Such adaptations can alter the temperature sensitivity (Q_{10}) of N transformations, yet most Earth system models simulate these processes using empirical enzyme-kinetic equations (for example, Michaelis–Menten) with fixed Q_{10} values. Similarly, while field experiments demonstrate that warming can enhance microbial decomposition, increase

plant-derived carbon inputs, and promote more efficient use of complex substrates, models often predict accelerated substrate depletion that suppresses subsequent mineralization (28, 43). As a result, models tend to underestimate the magnitude of N cycle responses to warming (44).

Another key source of discrepancy lies in the spatial and temporal scale of observation. Field experiments, often limited to small plots, may fail to capture long-term or landscape-level responses of vegetation and microbial communities to warming. Field experiments also tend to avoid extreme water stress or nutrient limitation (intentionally or unintentionally). In contrast, Earth system models incorporate large-scale carbon–nitrogen interactions and vegetation feedback, which can accentuate substrate (particularly nitrogen) limitation and attenuate warming responses. Moreover, the different time scales of observation might create some discrepancies, and the ecosystem models may have more compensating processes represented due to long time scale. In essence, current models may miss key microbial mechanisms but can capture broader ecosystem feedbacks operating at regional to global scales.

Moreover, *SI Appendix*, Fig. S4 shows the air and soil warming magnitudes in experiments and model simulations. Although significant differences between air and soil warming are evident in both cases, soil temperature responses in the model exhibit substantially greater variability. This variability arises because warming-induced increases in evapotranspiration, changes in soil moisture, and vegetation-mediated energy redistribution can offset or even exceed direct atmospheric heating at the soil surface. Such effects can, in turn, contribute to the observed discrepancies between model-based and experimental estimates of warming responses.

The Warming Response Depends On Soil Moisture But in Different Ways for N_2O, Mineralization, and Nitrification. Soil moisture is a key regulator of terrestrial N cycling, exerting strong control over N transformation processes and governing the production and release of soil greenhouse gases such as N_2O (45). Warming frequently alters soil moisture dynamics. A synthesis of published studies (*SI Appendix*, Fig. S5) indicates that elevated temperatures typically reduced soil water content (SWC) by 2.2% (The average soil depth is 9.6 cm). However, in high-elevation and high-latitude ecosystems, such as permafrost peatlands and tundra, warming may have neutral or even positive effects on SWC. To disentangle the role of hydrological shifts in modulating N cycling, we explicitly assessed both the absolute SWC (in the control) and warming-induced change in SWC (ΔSWC). Our model selection analyses (Fig. 2 *A–C*) identified ΔSWC as a key predictor of the RR of N_2O emissions, mineralization, and nitrification rates. Ecosystem type also emerged as a significant factor regulating the response of N_2O fluxes. Regression analyses revealed a clear nonlinear response of both mineralization and nitrification to ΔSWC: Rates increased with rising ΔSWC up to a peak at ΔSWC = 0, then declined beyond this threshold (Fig. 2 *E* and *F*). In addition, the responses of N_2O emissions and nitrification rates (Fig. 2 *G* and *I*) increased significantly with greater warming magnitudes; the responses of N mineralization rates (Fig. 2*K*) increased significantly with longer warming durations. The patterns revealed by these regressions show how the duration and magnitude of warming affect the key indicators of the N cycle—the warming effects on nitrogen transformations are sustained and may intensify with continued warming.

To characterize the baseline soil wetness across sites, we used the Aridity Index (AI)—defined as the ratio of mean annual precipitation to mean annual potential evapotranspiration (46) (*SI Appendix*, Table S2). This metric enabled us to assess the biogeographic patterns of N indicators along a continuous aridity gradient, ranging from hyperarid to humid regions, and to elucidate the mechanistic links between N dynamics and soil moisture regimes. By calculating the Pearson correlation coefficients and multiple linear regression results between the Aridity Index (AI) and three key indicators (the response ratio of N_2O emissions, N mineralization, and nitrification rates) under 2 and 4 °C warming scenarios, we found that the response ratio of nitrification rates was most strongly and positively correlated with AI, indicating that wetter regions tend to exhibit higher nitrification responses. In contrast, AI showed weaker negative correlations with the responses of both mineralization rates and N_2O emissions (*SI Appendix*, Fig. S6 *A* and *C*). Across different aridity zones, semiarid regions showed the strongest positive correlations between AI and all three N indicators, while arid regions showed the strongest negative correlations. Moreover, changes in the responses of mineralization and nitrification rates along the AI gradient were generally more pronounced than those observed for the response of N_2O emissions (*SI Appendix*, Fig. S6 *B* and *D*). These findings were further corroborated by the results of a Geographically Weighted Regression (GWR) model (*SI Appendix*, Fig. S6*E*), which were consistent with both the Pearson correlation and multiple regression analyses, reinforcing the robustness of our conclusions. A similar divergence was observed in the metaregression results: The response of N_2O emissions was not significantly correlated with either baseline SWC or ΔSWC, whereas the responses of both N mineralization and nitrification rates showed significant associations with ΔSWC but not with SWC (Fig. 2 *D–F* and *SI Appendix*, Table S3).

In conclusion, the response of N mineralization was primarily influenced by ΔSWC, while nitrification was affected by both ΔSWC and AI. In contrast, the response of N_2O emissions showed no significant relationship with either ΔSWC or SWC (baseline soil moisture conditions). This is a noteworthy finding: N mineralization is a microbially mediated decomposition process that is highly sensitive to soil moisture dynamics. It is more strongly influenced by intrinsic factors such as baseline soil organic matter content and microbial community composition, while being relatively less affected by long-term climatic conditions (47, 48). The alternating wetting-drying effects, resulting from fluctuations in soil moisture, can regulate the turnover of soil aggregates, release protected organic matter, and simultaneously modulate microbial activity, thereby triggering N mineralization (49, 50). Nitrification is governed by both short-term soil moisture changes and long-term climatic aridity. As aridity intensifies, decreasing soil water content enhances soil aeration and promotes substrate diffusion, creating conditions favorable for nitrification (51). Lower AI values are associated with higher oxygen availability, further facilitating nitrification (14, 52). Concurrently, drought stress suppresses plant transpiration, reduces N uptake by roots, and leads to N accumulation in soil—further stimulating nitrification (53, 54). With the projected increases in drought frequency and severity under future climate scenarios, together with subsequent wetting events that induce drying–rewetting cycles, the risks of nitrate leaching and N_2O emissions in arid regions may increase, particularly in nitrogen-saturated ecosystems. This highlights the need for targeted ecological management and improved predictive models (55, 56). N_2O emissions can result from both nitrification (aerobic) and denitrification (anaerobic). A decrease in soil water content favors nitrification, while an increase promotes denitrification. In our dataset, these opposing mechanisms may have counteracted one another, obscuring any significant correlation between N_2O fluxes and either SWC or ΔSWC. Moreover, N_2O emissions may only occur within specific soil moisture thresholds. For instance, previous studies have

shown that when soil pore water content exceeds 60%, net nitrification rates decline significantly (57). It is possible that the meta-analysis data did not sufficiently capture this critical moisture range, thereby obscuring any detectable relationship between N_2O emissions and soil moisture.

Warming Leads to a More Open Nitrogen Cycling. The natural abundance of the stable N isotope ($\delta^{15}N$) is a key indicator of ecosystem N dynamics and availability (58). Our analysis reveals that warming significantly increases $\delta^{15}N$ in both soils (+14.6%) and foliage (+14.9%) (Fig. 1 *B* and *C*). This isotopic enrichment suggests that warming accelerates N cycling by promoting the preferential loss of lighter ^{14}N, thereby leaving a residual N pool enriched in the heavier ^{15}N. Higher foliar $\delta^{15}N$ is generally interpreted as reflecting greater nitrogen availability to plants, and thus potentially reduced nitrogen limitation (59, 60).

Model selection analysis further shows that changes in soil and foliar $\delta^{15}N$ are primarily driven by shifts in ΔSWC and ΔT (*SI Appendix*, Fig. S7 *A* and *B*). Our metaregression analyses revealed that soil $\delta^{15}N$ increased linearly with both MAT and MAP across experimental sites independent of warming (*SI Appendix*, Fig. S7 *C* and *D*). Conversely, foliar $\delta^{15}N$ exhibited a significant nonlinear increase with ΔT (*SI Appendix*, Fig. S7*E*). It also displayed a unimodal relationship with MAP—initially decreasing and then increasing—with a turning point at 887 mm of annual precipitation (*SI Appendix*, Fig. S7*F*).

Different Responses of Soil and Plant Nitrogen to Warming. Experimental warming led to significant increases in soil inorganic N (+7.2%), nitrate (+10.9%), and ammonium (+8.3%) (Fig. 1*B*), but had no discernible impact on N concentrations in whole plants or individual organs (including leaves, roots, stems, litter, and shoots) (Fig. 1*C*). Warming-effects on soil N metrics were shaped by multiple factors (*SI Appendix*, Fig. S8), including ΔSWC, soil depth, warming magnitude, and warming method. In contrast, N concentrations in plants and leaves were primarily driven by ΔSWC alone. Regression analyses further revealed nonlinear responses of both soil and plant N variables to ΔT and duration (*SI Appendix*, Fig. S9).

These widespread nonlinear responses suggest that N dynamics under warming are governed by temporally shifting mechanisms. In the early stages of warming, accelerated N cycling may result from increased abundance of functional genes (e.g., *nirK*, *nirS*, *nifH*) associated with N transformation, enhancing decomposition, N availability, and plant productivity (61). However, such initial acceleration can give way to later-stage constraints, as labile substrate pools are progressively depleted, microbial communities undergo thermal acclimation and functional restructuring (41), and the system may transition into coupled abiotic–biotic feedback loops that alter soil thermal regimes and restructure microbial communities and their activity patterns (62, 63). In addition, early reductions in foliar and plant N concentrations may reflect a dilution effect, whereby warming stimulates plant growth and biomass accumulation, redistributing N into newly formed tissues—even as total N per plant increases (64). Alternatively, such nonlinearity may emerge from the aggregate response of distinct temperature-sensitive processes becoming sequentially prominent over time.

Subgroup analyses (*SI Appendix*, Figs. S10 and S11) showed no significant differences in the warming responses of soil and plant N metrics across ecosystem types. In contrast, warming methods showed more pronounced effects (*SI Appendix*, Figs. S11 and S12): Snow fence warming most consistently led to the greatest increases in soil inorganic N. Given that snow fences are primarily applied in cold-region ecosystems such as tundra and permafrost zones, this finding suggests that future climate warming may disproportionately alter N cycling in high-latitude and high-elevation environments, where N availability is often a critical constraint on productivity.

Caveats and Conclusions

Despite extensive research on the impacts of warming on N cycling, critical limitations still exist in uneven spatial distribution of study sites (*SI Appendix*, Fig. S13) and insufficient understanding of the interactive effects among multiple global change drivers. To overcome these bottlenecks, we call for more field-based research beyond the well-studied continents and ecosystems, and the development and implementation of more factorial experimental designs that explicitly test multidriver interactions. Meanwhile, the documentation of basic experimental and site information should be more consistent and comprehensive.

To our knowledge, this study established the most comprehensive global dataset to date and systematically explored the responses of terrestrial ecosystem N cycling to field warming from four key perspectives: N fluxes, N transformation processes, soil N, and plant N. It distinguished and elucidated the differing influences of soil water content (SWC) and changes in soil water content (ΔSWC) on the responses of N_2O emissions, N mineralization, and nitrification rates. Moreover, the study demonstrates that terrestrial nitrogen cycling is more dynamic under climate warming than previously recognized, highlighting the importance of integrating multiple analytical approaches to synthesize cross-scale ecological data.

Materials and Methods

Data Screening. The meta-analysis dataset was compiled with peer-reviewed papers published before September 2024, retrieved from the Web of Science, Scopus, ScienceDirect, Wiley Online Library, Springer Link, and China National Knowledge Infrastructure. The literature search employed the following terms: a) ("effect of temperature" OR "warming" OR "increas* temperature" OR "eleva* temperature") AND b) ("soil" OR "land" OR "terrestrial ecosystem") AND c) ("inorganic nitrogen" OR "inorganic N" OR "total nitrogen" OR "total N" OR "soil nitrogen" OR "soil N" OR "microbial biomass nitrogen" OR "MBN" OR "available nitrogen" OR "available N" OR "nitrate nitrogen" OR "nitric nitrogen" OR "nitrate-N" OR "NO_3^-" OR "NH_4^+" OR "ammonium nitrogen" OR "ammonium N" OR "nitrogen fixation" OR "N fixation" OR "nitrogen mineralization" OR "N mineralization" OR "nitrification" OR "nitration" OR "denitrification" OR "N_2O" OR "nitrous oxide" OR "N/P" OR "N:P" OR "dissolved organic nitrogen" OR "dissolved organic N" OR "DON"). To ensure accurate and effective literature screening, the following inclusion criteria were applied: 1) Only ecosystem-scale field warming manipulation experiments were included; pot experiments, laboratory incubations, elevational translocation experiments, geothermal warming, and model simulations were excluded. 2) The experimental design included at least one pair of treatments with the same conditions under warming and control treatments. 3) At least one N cycling variable (e.g., N pools, fluxes, or dynamics) was reported. 4) Definite replicate numbers must be provided. A PRISMA 2020 flow diagram is provided in *SI Appendix*, Fig. S14, and a PRISMA 2020 Checklist is included as a separate supplementary document.

Data Collection. When a study reported multiple sampling dates, data were treated as separate entries if the interval between sampling dates exceeded half a year. If the interval was less than half a year, only the most recent sampling date was used (65). For studies with multiple warming treatments (e.g., different warming magnitudes or methods), each treatment was recorded separately. In a few cases, data were reported separately for growing and nongrowing seasons but without clearly defined cutoff dates. In such cases, we subjectively divided the seasons based on local climatic conditions. Most of the data included in this study came from year-round continuous warming experiments (except for the snow fence). Other seasonal or intermittent warming treatments were rarely reported

and thus were not analyzed separately. For studies presenting data as boxplots without reporting mean values, we estimated the means following the method of Shi et al. (66).

We recorded soil and air warming magnitudes, together with soil warming depth and air measurement height. When both air and soil warming magnitudes were reported, soil warming magnitude was used to characterize warming intensity; when only one was reported, that value was used. For studies reporting separate daytime and nighttime warming magnitudes, we used the average of the two. Similarly, when warming magnitude varied seasonally (e.g., enhanced winter warming treatments), we averaged across seasons. In cases where the designed warming magnitude differed from the measured magnitude, we used the measured value obtained from temperature sensors. We prioritized the use of mean annual soil warming magnitudes, and if not available, used values for the growing season or the sampling month, in that order of preference. In addition, to ensure the reliability of the dataset, we excluded studies reporting negative soil warming magnitudes, which commonly occur in cold ecosystems such as tundra and subarctic shrublands. Based on the above criteria, a total of 7,941 observations from 413 publications were included in the final dataset (see *SI Appendix*, Table S4 for details on the included indicators and their distribution). Numeric data were extracted from figures using GetData Graph Digitizer 2.22. Missing mean annual temperature (MAT) and mean annual precipitation (MAP) values were filled by querying WorldClim using the *geodata* R package.

Overview of Global Warming Manipulative Experiments. Through a comprehensive literature search, we compiled 7,941 observations from 413 peer-reviewed publications encompassing all major terrestrial ecosystems worldwide (see Supplementary Reference List and *SI Appendix*, Table S5 for detailed information). Most of the experiments were conducted in Asia, Europe, and North America, with a small number located in Oceania, South America, and Antarctica. Notably, no qualifying studies were found from Africa (*SI Appendix*, Fig. S13*A*). Among the 438 experimental sites, grasslands were the most frequently studied ecosystem type (175 sites, 40%), followed by forests (90 sites, 21%), croplands (63 sites, 14%), and tundra (44 sites, 10%). Other ecosystems (including heathland, peatland, shrubland, desert, swamp, and fellfield) were relatively underrepresented, with only 29, 12, 13, 6, 4, and 2 sites, respectively, despite their potentially high sensitivity to climate warming (67).

To characterize site conditions, we compiled available climatic indicators such as MAT (ranging from −20 to 27 °C) and precipitation (81 to 2,128 mm), along with key soil properties including nutrient levels and soil water content (SWC). We also extracted experimental design variables, including warming magnitude (0.01 to 7.52 °C), duration (0.08 to 28 y), and warming method, which were categorized into five types: open-top chamber (OTC, 180 sites), infrared radiator (IR, 132 sites), heating cable (HC, 59 sites), snow fence (SF, 14 sites), and others (e.g., greenhouse, infrared reflective curtain (IRC), IR+HC, IRC+HC, and fleeces covering, 53 sites). Across all experiments, the average warming magnitude was 1.9 °C (*SI Appendix*, Fig. S13*C*), while SWC decreased by 2.2% compared to control plots (*SI Appendix*, Fig. S13*D*). The longest average experimental durations were observed in tundra (7.9 y), followed by other ecosystems (4.4 y) and grassland (3.2 y). Forest and cropland had the shortest average durations at 2.4 and 2.1 y, respectively (*SI Appendix*, Fig. S13*E*). To compile a more comprehensive dataset, this study also includes warming responses of several relatively understudied N metrics, along with associated carbon and phosphorus indicators (*SI Appendix*, Figs. S15–S17). These include variables such as N resorption rate, ammonification rate, and ^{15}N recovery, all of which hold unique ecological significance and deserve greater attention.

Meta-analysis. The natural logarithm of the response ratio (RR) was used as the effect size to quantify the impact of warming on nitrogen cycling variables, following Eq. **1** (68):

$$RR = \ln\left(\frac{X_t}{X_c}\right) = \ln X_t - \ln X_c, \quad [1]$$

where X_t and X_c are the mean values of the indicators under warming (t) and control (c) conditions, respectively. For indicators such as greenhouse gas emissions that may be negative, effect sizes were calculated using the method of Guo et al. (69). The weight for each data point was calculated using Eq. **2** (70, 71):

$$weight = \left(N_t \times N_c\right) / \left(N_t + N_c\right), \quad [2]$$

where N_t and N_c are the number of replicates for the treatment and control groups, respectively.

Meta-analysis was conducted with *lme4* package (72) to assess the overall effect of warming on N cycling indicators. To account for the dependence of multiple observations in the same study, we added "site" as random factors into the meta-analysis model. If the 95% CI did not overlap zero, the estimated effect was considered significant; otherwise, it was considered insignificant (73). Metaregressions were performed to explore relationships between the RR of N variables and the RR of environmental variables (74).

We also conducted model selection analysis to evaluate the relative importance of multiple factors influencing N cycling responses to warming. The relative importance of each predictor was defined as the sum of the Akaike weights across all models that included the predictor, indicating the overall support for that predictor. Following the approach of Terrer et al. (75), we used 0.8 as the threshold: Variables with importance scores >0.8 were considered significant, while those <0.8 were considered nonessential. In this study, we explored the relative importance of the MAT, MAP, soil depth, experimental duration, warming method, warming magnitude (ΔT), change of soil water content (ΔSWC) and ecosystem type using the *glmulti* package (76).

Begg's and Egger's tests were used to detect publication bias, with significance defined as $p < 0.05$ (77, 78). As shown in *SI Appendix*, Table S6, no significant publication bias was detected. The natural abundance of the stable nitrogen isotope ($\delta^{15}N$) is calculated as $\delta^{15}N = \left(R_{sample}/R_{standard} - 1\right) \times 1{,}000$ (‰), where R_{sample} and $R_{standard}$ denote the $^{15}N/^{14}N$ ratios in the sample and atmospheric nitrogen, respectively (79, 80). All analyses were conducted in R version 4.4.1 (81).

Global Mapping. To further investigate the global spatial patterns of warming effects on key N cycling processes, we developed a random forest regression model to upscale our meta-analysis findings from site level to the global scale, with projections representing late-century conditions (2080 to 2100). The meta-analysis effect size (natural log response ratio, lnRR) was used as the response variable. Eight climatic and soil predictors were selected: MAT and precipitation (MAP), warming magnitude and duration, soil total N content, soil carbon-to-nitrogen ratio (C:N), soil pH, and soil moisture content. Using this predictor set, the trained model was applied to simulate spatially explicit changes in N_2O emission rates, soil N mineralization rates, and nitrification rates under +2 and +4 °C warming scenarios. Soil property data (total N, C:N ratio, pH, and moisture content) were obtained from the Harmonized World Soil Database v2.0 (HWSD, https://gaez.fao.org/pages/hwsd), while MAT and MAP were obtained from WorldClim v2.1 (https://www.worldclim.org/data/worldclim21.html). All data were resampled to a spatial resolution of 0.042° × 0.042° to match the modeling framework. Final global predictions were also produced at 0.042° × 0.042° resolution, resulting in high-resolution maps of warming impacts on nitrogen cycling processes. In addition, we also developed a random forest regression model at a resolution of 1.9° × 2.5° for comparison with the CLM results (*SI Appendix*, Fig. S18). The results of the mapping under the two resolutions are similar (Fig. 4).

The data processing workflow proceeded as follows. First, we cleaned the meta-analysis dataset by 1) retaining only observations with nonmissing effect sizes, 2) excluding treatments involving interaction effects, 3) removing entries lacking soil depth information, and 4) excluding soil-only warming experiments and retaining only those imposing simultaneous air and soil warming, to improve the comparability between the global mapping results and the CLM simulations. For records with missing values, we used multidepth data from HWSD to fit vertical soil profiles and implemented depth-specific interpolation to impute missing pedological indicators. The dataset was then split into 80% training and 20% validation subsets. Key random forest hyperparameters (e.g., number of trees, maximum depth) were optimized via cross-validation. Model performance was evaluated based on the coefficient of determination (R^2), mean absolute error (MAE), and Rms error (RMSE) to assess the accuracy of upscaled predictions against observed warming responses in the validation dataset. The ten-fold cross-validation results for upscaling models of three key N cycle indicators are shown in *SI Appendix*, Fig. S19, and the random forest feature contributions plot is shown in *SI Appendix*, Fig. S20. To quantify and account for the inherent uncertainties in our spatial predictions, we employed a Monte Carlo simulation. The trained random forest model was run for 100 iterations, and the final global

maps were generated by taking the average of the 100 simulation outputs. The SD across the 100 runs was also calculated.

CLM. We used the CLM version 5.0 with Biogeochemistry (CLM5-BGC) embedded in the Community Earth System Model version 2.2 (CESM2.2, https://github.com/ESCOMP/CESM) as the core numerical platform. The model was configured with the I2000Clm50BgcCruGs compset, which activates fully coupled dynamic carbon–nitrogen cycling, making it suitable for biogeochemical studies.

The simulations were conducted globally at a spatial resolution of 1.9° × 2.5°. The climate forcing was derived from the 2000-y climatology of the CRU TS4.05 reanalysis dataset. This single-year record was cycled repeatedly to maintain temporal consistency and align with the WorldClim v2.1 baseline. Land use, N deposition, and atmospheric CO_2 levels were held constant to isolate the independent effects of temperature change.

Warming scenarios were implemented via uniform increases of +2 and +4 °C in near-surface air temperature relative to the control simulation representing historical conditions (circa year 2000 baseline), while keeping other meteorological variables (e.g., precipitation, radiation) unchanged, thereby inducing simultaneous warming of both aboveground and belowground components. Each simulation (+2 °C, +4 °C) was run for 100 y. Steady state was considered reached when the annual rate of change in soil organic carbon storage fell below 1%. The first 10 y were treated as spin-up and discarded. The final results were based on the average values over the 20-y period from 2080 to 2100, focusing on interannual variability in N_2O emission flux, net N mineralization rate, and nitrification rate, with the associated SD calculated to quantify model uncertainty during this timeframe. All simulations were executed on the FusionOne high-performance computing cluster at the High-Performance Computing Center of Peking University. Paired samples T-tests were also conducted to determine whether the changes of three nitrogen cycle parameters were statistically significant between warming scenarios (82).

Data, Materials, and Software Availability. The meta-analysis data and code that support the findings of this study are openly available in Mendeley (83). Soil property data were obtained from the Harmonized World Soil Database v2.0 (84). Mean annual temperature (MAT) and mean annual precipitation (MAP) data were sourced from WorldClim version 2.1 (85). The Community Land Model (CLM) forcing data are available at ref. 86. The Global Evapotranspiration (ET) and Aridity Index Database can be accessed via Figshare (87).

ACKNOWLEDGMENTS. We sincerely thank all the scientists whose data and work were included in this meta-analysis. Special thanks go to William Riley (Lawrence Berkeley National Laboratory), Lei Zhang (Lawrence Berkeley National Laboratory), and Shengwen Xu (Wuhan Institute of Technology) for their suggestions on this study. This study was financially supported by the National Natural Science Foundation of China (32425038 and 32588202) and the State Key Laboratory of Vegetation Structure, Function and Construction (Project No: VegLab2025002).

Author affiliations: [a]Ministry of Education Key Laboratory of Ecology and Resource Use of the Mongolian Plateau, Inner Mongolia Key Laboratory of Grassland Ecology, and School of Ecology and Environment, Inner Mongolia University, Hohhot 010021, China; [b]State Key Laboratory of Vegetation Structure, Function and Construction (VegLab), Ministry of Education Key Laboratory of Earth Surface Processes, and College of Urban and Environmental Sciences, Peking University, Beijing 100871, China; [c]College of Natural Resources and Environment, Northwest A&F University, Yangling 712100, China; [d]Department of Ecology, Evolution and Marine Biology, University of California, Santa Barbara, CA 93106; [e]Climate and Ecosystem Sciences Division, Lawrence Berkeley National Laboratory, Berkeley, CA 94720; and [f]Energy and Resources Group, University of California, Berkeley, CA 94720

Author contributions: B.Z. designed research; X.W. and C.N. performed research; Z.F., W.W., C.X., J.F., and R.Y. contributed new reagents/analytic tools; X.W. and C.N. analyzed data; B.Z. secured funding; and X.W., C.N., J.P.S., M.S.T., and B.Z. wrote the paper.

1. J. N. Galloway, A. Bleeker, J. W. Erisman, The human creation and use of reactive nitrogen: A global and regional perspective. *Annu. Rev. Environ. Resour.* **46**, 255–288 (2021).
2. R. Barnard, P. W. Leadley, B. A. Hungate, Global change, nitrification, and denitrification: A review. *Glob. Biogeochem. Cycles* **19**, GB1007 (2005).
3. R. E. Mason *et al.*, Evidence, causes, and consequences of declining nitrogen availability in terrestrial ecosystems. *Science* **376**, 261 (2022).
4. J. Y. Lee *et al.*, "Future global climate: scenario-based projections and near-term information" In *Climate Change 2021: The Physical Science Basis. Contribution of Working Group I to the Sixth Assessment Report of the Intergovernmental Panel on Climate Change*, V. Masson-Delmotte, Eds. (Cambridge University Press, Cambridge, United Kingdom and New York, NY, USA, 2021), pp. 553–672.
5. P. Forster *et al.*, "The earth's energy budget, climate feedbacks, and climate sensitivity" in *Climate Change 2021: the Physical Science Basis. Contribution of Working Group I to the Sixth Assessment Report of the Intergovernmental Panel On Climate Change*, (Cambridge University Press, Cambridge, United Kingdom and New York, NY, USA, 2021), pp. 923–1054.
6. H. Tian *et al.*, Global nitrous oxide budget (1980–2020). *Earth Syst. Sci. Data* **16**, 2543–2604 (2024).
7. M. M. Turner, H. A. L. Henry, Net nitrogen mineralization and leaching in response to warming and nitrogen deposition in a temperate old field: The importance of winter temperature. *Oecologia* **162**, 227–236 (2010).
8. J. Leppälammi-Kujansuu *et al.*, Effects of long-term temperature and nutrient manipulation on Norway spruce fine roots and mycelia production. *Plant Soil* **366**, 287–303 (2013).
9. M. A. Dawes, P. Schleppi, S. Hattenschwiler, C. Rixen, F. Hagedorn, Soil warming opens the nitrogen cycle at the alpine treeline. *Glob. Change Biol.* **23**, 421–434 (2017).
10. W. Gao, D. Yan, Warming suppresses microbial biomass but enhances N recycling. *Soil Biol. Biochem.* **131**, 111–118 (2019).
11. M. Olsrud, B. A. Carlsson, B. M. Svensson, A. Michelsen, J. M. Melillo, Responses of fungal root colonization, plant cover and leaf nutrients to long-term exposure to elevated atmospheric CO_2 and warming in a subarctic birch forest understory. *Glob. Change Biol.* **16**, 1820–1829 (2010).
12. P. L. Sorensen, A. Michelsen, Long-term warming and litter addition affects nitrogen fixation in a subarctic heath. *Glob. Change Biol.* **17**, 528–537 (2011).
13. E. Bai *et al.*, A meta-analysis of experimental warming effects on terrestrial nitrogen pools and dynamics. *New Phytol.* **199**, 441–451 (2013).
14. R. Liu *et al.*, The effect of temperature and moisture on the source of N_2O and contributions from ammonia oxidizers in an agricultural soil. *Biol. Fertil. Soils* **53**, 141–152 (2016).
15. S. Jonasson, M. Havström, M. Jensen, T. V. Callaghan, In situ mineralization of nitrogen and phosphorus of Arctic soils after perturbations simulating climate change. *Oecologia* **95**, 179–186 (1993).
16. W. T. Peterjohn, J. M. Melillo, F. P. Bowles, P. A. Steudler, Soil warming and trace gas fluxes: Experimental design and preliminary flux results. *Oecologia* **93**, 18–24 (1993).
17. S. Liu *et al.*, Increased soil release of greenhouse gases shrinks terrestrial carbon uptake enhancement under warming. *Glob. Change Biol.* **26**, 4601–4613 (2020).
18. A. Salazar, K. Rousk, I. S. Jónsdóttir, J. P. Bellenger, O. S. Andrésson, Faster nitrogen cycling and more fungal and root biomass in cold ecosystems under experimental warming: A meta-analysis. *Ecology* **101**, e02938 (2020).
19. Z. Dai *et al.*, Elevated temperature shifts soil N cycling from microbial immobilization to enhanced mineralization, nitrification and denitrification across global terrestrial ecosystems. *Glob. Change Biol.* **26**, 5267–5276 (2020).
20. Y. K. Kim, J. Hyun, A. Michelsen, E. E. Kwon, J. Y. Jung, Key determinants of soil labile nitrogen changes under climate change in the Arctic: A meta-analysis of the responses of soil labile nitrogen pools to experimental warming and snow addition. *Chem. Eng. J.* **494**, 153066 (2024).
21. Y. Sun *et al.*, A global meta-analysis on the responses of C and N concentrations to warming in terrestrial ecosystems. *Catena* **208**, 105762 (2022).
22. M. Zheng *et al.*, Warming promotes nitrogen and carbon cycles in global grassland. *Environ. Sci. Technol.* **59**, 2505–2518 (2025).
23. M. Gödde, R. Conrad, Immediate and adaptational temperature effects on nitric oxide production and nitrous oxide release from nitrification and denitrification in two soils. *Biol. Fertil. Soils* **30**, 33–40 (1999).
24. T. J. Griffis *et al.*, Nitrous oxide emissions are enhanced in a warmer and wetter world. *Proc. Natl. Acad. Sci. U.S.A.* **114**, 12081–12085 (2017).
25. L. E. Rustad *et al.*, A meta-analysis of the response of soil respiration, net nitrogen mineralization, and aboveground plant growth to experimental ecosystem warming. *Oecologia* **126**, 543–562 (2001).
26. X. S. Tu *et al.*, Warming-induced stimulation of soil N_2O emissions counteracted by elevated CO_2 from nine-year agroecosystem temperature and free air carbon dioxide enrichment. *Environ. Sci. Technol.* **58**, 6215–6225 (2024).
27. H. Gao, H. Tian, Z. Zhang, X. Xia, Warming-induced greenhouse gas fluxes from global croplands modified by agricultural practices: A meta-analysis. *Sci. Total Environ.* **820**, 153288 (2022).
28. E. A. Davidson, I. A. Janssens, Temperature sensitivity of soil carbon decomposition and feedbacks to climate change. *Nature* **440**, 165–173 (2006).
29. S. D. Frey, J. Lee, J. M. Melillo, J. Six, The temperature response of soil microbial efficiency and its feedback to climate. *Nat. Clim. Chang.* **3**, 395–398 (2013).
30. C. Bamminger, C. Poll, S. Marhan, Offsetting global warming-induced elevated greenhouse gas emissions from an arable soil by biochar application. *Glob. Change Biol.* **24**, 318–334 (2018).
31. M. E. Marushchak *et al.*, Hot spots for nitrous oxide emissions found in different types of permafrost peatlands. *Glob. Change Biol.* **17**, 2601–2614 (2011).
32. S. E. Ward *et al.*, Warming effects on greenhouse gas fluxes in peatlands are modulated by vegetation composition. *Ecol. Lett.* **16**, 1285–1293 (2013).
33. K. Butterbach-Bahl, E. M. Baggs, M. Dannenmann, R. Kiese, S. Zechmeister-Boltenstern, Nitrous oxide emissions from soils: How well do we understand the processes and their controls?. *Philos. Trans. R. Soc. B-Biol. Sci.* **368**, 20130122 (2013).
34. M. S. Carter *et al.*, Effects of elevated atmospheric CO_2, prolonged summer drought and temperature increase on N_2O and CH_4 fluxes in a temperate heathland. *Soil Biol. Biochem.* **43**, 1660–1670 (2011).
35. M. E. Marushchak *et al.*, Thawing yedoma permafrost is a neglected nitrous oxide source. *Nat. Commun.* **12**, 7107 (2021).
36. M. Rantanen *et al.*, The arctic has warmed nearly four times faster than the globe since 1979. *Commun. Earth Environ.* **3**, 1–10 (2022).
37. M. E. Repo *et al.*, Large N_2O emissions from cryoturbated peat soil in tundra. *Nat. Geosci.* **2**, 189–192 (2009).
38. M. A. Adams, T. L. Turnbull, J. I. Sprent, N. Buchmann, Legumes are different: Leaf nitrogen, photosynthesis, and water use efficiency. *Proc. Natl. Acad. Sci. U.S.A.* **113**, 4098–4103 (2016).
39. H. Chen *et al.*, Topography modulates effects of nitrogen deposition on microbial resource limitation in a nitrogen-saturated subtropical forest. *For. Ecosyst.* **8**, 68 (2021).

40. K. G. Sian, M. Duncan, Nitrogen-fixing trees increase soil nitrous oxide emissions: A meta-analysis. *Ecology* **102**, e03415 (2021).
41. J. M. Melillo *et al.*, Long-term pattern and magnitude of soil carbon feedback to the climate system in a warming world. *Science* **358**, 101–104 (2017).
42. A. T. Nottingham *et al.*, Microbial diversity declines in warmed tropical soil and respiration rise exceed predictions as communities adapt. *Nat. Microbiol.* **7**, 1650 (2022).
43. L. Cheng *et al.*, Warming enhances old organic carbon decomposition through altering functional microbial communities. *ISME J.* **11**, 1825–1835 (2017).
44. K. E. O. Todd-Brown *et al.*, Changes in soil organic carbon storage predicted by Earth system models during the 21st century. *Biogeosciences* **11**, 2341–2356 (2014).
45. J. Liao *et al.*, Soil moisture–atmosphere feedback dominates land N_2O nitrification emissions and denitrification reduction. *Glob. Change Biol.* **28**, 6404–6418 (2022).
46. R. J. Zomer, J. Xu, A. Trabucco, Version 3 of the global aridity index and potential evapotranspiration database. *Sci. Data* **9**, 409 (2022).
47. W. H. Schlesinger, J. A. Raikes, A. E. Hartley, A. E. Cross, On the spatial pattern of soil nutrients in desert ecosystems. *Ecology* **77**, 364–374 (1996).
48. J. Zhang, Z. Cai, C. Muller, Terrestrial N cycling associated with climate and plant-specific N preferences: A review. *Eur. J. Soil Sci.* **69**, 488–501 (2018).
49. S. Liu *et al.*, Drying-wetting cycles affect soil structure by impacting soil aggregate transformations and soil organic carbon fractions. *Catena* **243**, 108188 (2024).
50. S. Manzoni, J. P. Schimel, A. Porporato, Responses of soil microbial communities to water stress: Results from a meta-analysis. *Ecology* **93**, 930–938 (2012).
51. J. Ren *et al.*, Dryland watersheds in flux: How nitrogen deposition and changing precipitation regimes shape nitrogen export? *Earth's Future* **12**, e2023EF004120 (2024).
52. R. E. Drenovsky, D. Vo, K. J. Graham, K. M., Scow Soil water content and organic carbon availability are major determinants of soil microbial community composition. *Microb. Ecol.* **48**, 424–430 (2004).
53. J. M. Stark, M. K. Firestone, Mechanisms for soil-moisture effects on activity of nitrifying bacteria. *Appl. Environ. Microbiol.* **61**, 218–221 (1995).
54. J. F. Weltzin *et al.*, Assessing the response of terrestrial ecosystems to potential changes in precipitation. *BioScience* **53**, 941–952 (2003).
55. A. Tietema *et al.*, Nitrate leaching in coniferous forest ecosystems: The European field-scale manipulation experiments NITREX (nitrogen saturation experiments) and EXMAN (experimental manipulation of forest ecosystems). *Glob. Biogeochem. Cycle* **11**, 617–626 (1997).
56. V. H. Klaus, L. Friedritz, U. Hamer, T. Kleinebecker, Drought boosts risk of nitrate leaching from grassland fertilization. *Sci. Total Environ.* **726**, 137877 (2020).
57. X. Dan, Z. Chen, Y. Cheng, Z. Cai, J. Zhang, Response of nitrogen transformations to moisture changing in red soil. *J. Zhejiang A&F Univ.* **38**, 896–905 (2021).
58. D. Robinson, $\delta^{15}N$ as an integrator of the nitrogen cycle. *Trends Ecol. Evol.* **16**, 153–162 (2001).
59. J. M. Craine *et al.*, Global patterns of foliar nitrogen isotopes and their relationships with climate, mycorrhizal fungi, foliar nutrient concentrations, and nitrogen availability. *New Phytol.* **183**, 980–992 (2009).
60. C. T. Garten, H. Van Miegroet, Relationships between soil nitrogen dynamics and natural ^{15}N abundance in plant foliage from Great Smoky Mountains National Park. *Can. J. For. Res.* **24**, 1636–1645 (1994).
61. S. E. Hobbie, F. S. Chapin, The response of tundra plant biomass, aboveground production, nitrogen, and CO_2 flux to experimental warming. *Ecology* **79**, 1526–1544 (1998).
62. J. R. Deslippe, M. Hartmann, S. W. Simard, W. W. Mohn, Long-term warming alters the composition of Arctic soil microbial communities. *FEMS Microbiol. Ecol.* **82**, 303–315 (2012).
63. S. A. Sistla *et al.*, Long-term warming restructures Arctic tundra without changing net soil carbon storage. *Nature* **497**, 615-+ (2013).
64. F. S. Chapin, G. R. Shaver, A. E. Giblin, K. J. Nadelhoffer, J. A. Laundre, Responses of Arctic tundra to experimental and observed changes in climate. *Ecology* **76**, 694–711 (1995).
65. X. Wang *et al.*, Minor effects of warming on soil microbial diversity, richness and community structure. *Glob. Change Biol.* **31**, e70104 (2025).
66. J. Shi *et al.*, Optimally estimating the sample standard deviation from the five-number summary. *Res. Synth. Methods* **11**, 641–654 (2020).
67. W. Xing *et al.*, Climate controls on carbon accumulation in peatlands of Northeast China. *Quat. Sci. Rev.* **115**, 78–88 (2015).
68. L. V. Hedges, J. Gurevitch, P. S. Curtis, The meta-analysis of response ratios in experimental ecology. *Ecology* **4**, 1150–1156 (1999).
69. J. Guo *et al.*, Global climate change increases terrestrial soil CH4 emissions. *Glob. Biogeochem. Cycles* **37**, e2021GB007255 (2023).
70. C. Chen, H. Y. H. Chen, X. Chen, Z. Huang, Meta-analysis shows positive effects of plant diversity on microbial biomass and respiration. *Nat. Commun.* **10**, 1332 (2019).
71. C. M. Pittelkow *et al.*, Productivity limits and potentials of the principles of conservation agriculture. *Nature* **517**, 365–U482 (2015).
72. D. Bates, M. Maechler, B. M. Bolker, S. C. Walker, Fitting linear mixed-effects models using lme4. *J. Stat. Softw.* **67**, 1–48 (2015).
73. Z. Zhang, Y. Liu, L. Yuan, E. Weber, V. K. Mark, Effect of allelopathy on plant performance: A meta-analysis. *Ecol. Lett.* **24**, 348–362 (2020).
74. F. Hua *et al.*, The biodiversity and ecosystem service contributions and trade-offs of forest restoration approaches. *Science* **376**, 839-+ (2022).
75. C. Terrer, S. Vicca, B. A. Hungate, R. P. Phillips, I. C. Prentice, Mycorrhizal association as a primary control of the CO_2 fertilization effect. *Science* **353**, 72–74 (2016).
76. V. Calcagno, C. De Mazancourt, Glmulti: An R package for easy automated model selection with (generalized) linear models. *J. Stat. Softw.* **34**, 1–29 (2010).
77. M. Egger, S. G. Davey, M. Schneider, C. Minder, Bias in meta-analysis detected by a simple, graphical test. *BMJ-Brit. Med. J.* **315**, 629–634 (1997).
78. J. Koricheva, J. Gurevitch, K. L. Mengersen, *Handbook of Meta-analysis in Ecology and Evolution* (Princeton University Press, 2013).
79. Q. Chen *et al.*, Global mycorrhizal status drives leaf $\delta^{15}N$ patterns. *J. Ecol.* **113**, 1150–1163 (2025).
80. Z. Lie *et al.*, Warming leads to more closed nitrogen cycling in nitrogen-rich tropical forests. *Glob. Change Biol.* **27**, 664–674 (2021).
81. R Core Team, *R: A Language and Environment for Statistical Computing* (R Foundation for Statistical Computing, Vienna, Austria, 2024).
82. A. Ross, V. L. Willson, *Paired Samples t test//Basic and Advanced Statistical Tests: Writing Results Sections and Creating Tables and Figures* (Sense Publishers, Rotterdam, 2017), pp. 17–19.
83. X. Wang *et al.*, Data and code: Terrestrial ecosystem nitrogen cycling in response to field warming: Global patterns and future trends. Mendeley Data, V1. https://doi.org/10.17632/265nm6v26d.1. Deposited 11 January 2026.
84. Food and Agriculture Organization of the United Nations, Harmonized World Soil Database (HWSD) v2.0. Food and Agriculture Organization of the United Nations database. https://gaez.fao.org/pages/hwsd. Accessed 10 October 2025.
85. S. E. Fick, R. J. Hijmans, WorldClim 2: new 1km spatial resolution climate surfaces for global land areas. WorldClim. https://www.worldclim.org/data/worldclim21.html. Accessed 10 October 2025.
86. National Center for Atmospheric Research, Community Earth System Model (CESM) input data. NCAR database. https://ftp.cgd.ucar.edu/cesm/inputdata/. Accessed 10 October 2025.
87. R. Zomer, A. Trabucco, Global Aridity Index and Potential Evapotranspiration (ET0) Database: Version 3.1. Figshare. https://doi.org/10.6084/m9.figshare.7504448.v7. Deposited 17 July 2025.